PCCP

Accepted Manuscript

ROYAL SOCIETY OF CHEMISTRY

www.rsc.org/pccp

Journal Name

RSCPublishing

ARTICLE

Observations of Probe Dependence in the Solvation Dynamics in Ionic Liquids

Cite this: DOI: 10.1039/xoxxoooooox

Xin-Xing Zhang,[a,b*] Jens Breffke,[c] Nikolaus P. Ernsting,[b] and Mark Maroncelli[c*]

Received ooth January 2012,
Accepted ooth January 2012

DOI: 10.1039/xoxxoooooox

www.rsc.org/

Solvation and rotational dynamics of 4-aminophthalimide (4AP) in four ionic liquids (ILs) are measured using a combination of fluorescence upconversion spectroscopy and time-correlated single photon counting. These data are compared with previously reported data on coumarin 153 (C153) to investigate the probe dependence of solvation dynamics. No fast component (<15 ps) in the fluorescence anisotropy is observed with 4AP. The differences between the solvation response functions of 4AP and C153 are significant in all four ILs, but these differences can be reduced by applying a correction for solute rotation using measured emission anisotropies. Response functions of other probes available in the literature are used to further examine the validity of this correction. The corrected data are also compared to predictions of dielectric continuum models of solvation. By replacing the measured static conductivity of the ILs with an estimated value, such predictions show good agreement with the observed spectral response functions, especially when the anion size is small.

Introduction

Room-temperature ionic liquids (ILs) are low-melting salts with distinctive properties such as negligible vapor pressures at ambient temperatures, high ionic conductivities, and miscibility with both organic and inorganic solvents. These properties enable applications in many fields, including synthesis, analytical separations, as well as in important energy-related technologies, and pursuit of these applications has been vigorous over the past decade.[1-16] In support of this work, a vast amount of fundamental research, for example on dielectric relaxation and solvation dynamics, has also been published.[17-34] Solvation dynamics, energy relaxation in response to the charge redistribution of a solute, is an important determinant in regulating reaction rates and is of particular interest in the present work. Spectroscopic techniques such as fluorescence upconversion, [35-37] optical Kerr gating,[38] and three-pulse photon echo peak shift measurements[39] have been used to measure the solvation response of various solvatochromic probes in ILs. Systematic studies with diverse solutes have been reported by several groups in an effort to determine the sensitivity of dynamics to the choice of probe.[30, 40-47] Rotational dynamics of ILs have been found to be strongly dependent on the solute's polarity,[44, 48] however no significant influence of solute identity on the solvation response has been observed except where specific solute-solvent interactions were speculated to play a role.[30, 40, 42, 46, 47]

To understand molecular aspects of solvation, multiple groups have also performed molecular dynamics (MD) simulations of ionic liquids.[49-60] A series of pioneering simulations by Shim, Kim and coworkers,[49-52] primarily studying model diatomic solutes, first uncovered the pronounced biphasic character of the solvation response in ionic liquids and documented a number of important general features of ionic liquid solvation. In other early work, Kobrak and coworkers performed MD simulations of the experimental solutes betaine-30 and C153 in various ILs, focusing on the short-time dynamics.[54-56] More recent simulations of C153 solvation[57-60] have sought to make direct comparisons to experimental measurements and have shown that simulations with all-atom models can semi-quantitatively capture the dynamics observed experimentally.[58, 59] Several simulation studies have examined the relationship between solvation and dielectric relaxation in neat ionic liquids[51, 60] and have shown the same departures from dielectric continuum predictions of solvation dynamics observed experimentally.[35] Of particular interest in the present work is the role solute characteristics might play in determining solvation dynamics in ionic liquids. Shim and Kim[51] reported marked differences in solvation correlation functions of nonpolar and ion-pair diatomics, with the latter being nearly 8-fold faster.[61] Roy and Maroncelli[57] showed that much of this difference can be attributed to the effect fast rotation of the nonpolar solute has in speeding up the solvation. They also showed that the effects of

solute motion are non-negligible even for large solutes such as C153, where solute motion was found to increase the rate of solvation 2-fold in a coarse-grained model ionic liquid. Biswas and coworkers[62] also used a semi-molecular theory together with experimental dielectric data to show that both solute rotational and translational motions can serve to enhance solvation rates.

In the present work we augment our recent measurements of solvation dynamics with new data on the dynamic Stokes shift of 4-aminophthalimide (4AP) in four representative ionic liquids. The purpose was to determine whether 4AP reports solvation in ionic liquids differently than the C153 probe used in our previous studies. As in our past work,[35, 36] we combine femtosecond broadband fluorescence upconversion (FLUPS) and picosecond time-correlated single photon counting (TCSPC) measurements in order to capture the complete solvation response over the range 100 fs – 20 ns. We find systematic differences between the solvation response functions reported by these solutes. To explore whether these differences might be the result of solute motion as suggested by simulation[57] and theory,[62] we also measure the fluorescence anisotropy decay of 4AP in these ionic liquids. As recently found by Sajadi et al.[63] for a number of solutes in methanol, we find that "rotational correction" of the solvation response approximately reconciles the differences in the solvation response functions reported by the two probes. These results suggest that solvation dynamics in ionic liquids are indeed influenced by solute motion. We also consider what these results mean for tests of dielectric continuum models of solvation in ionic liquids.

Materials and Methods

4-Aminophthalamide (4AP) for fluorescence upconversion measurements was from Acros (97% purity) and used as received. 4AP obtained from Sigma-Aldrich was recrystallized from methanol + water (1:1 volume ratio) and used for time-correlated single photon counting measurements. Ionic liquids $[Im_{41}][DCA]$, $[Im_{41}][BF_4]$, $[Im_{41}][Tf_2N]$ and $[Pr_{41}][Tf_2N]$ were obtained from Iolitec and dried under vacuum for 20 hours at room temperature prior to use. Water contents of ILs were below 100 and 300 ppm by weight before and after the course of an experiment (approximately 5 hours), respectively. Their chemical names and CAS registry numbers are provided in Table 1.

Spectroscopic measurements and data analysis methods were the same as those described in detail in Ref.[35]. Briefly, Hitachi U-3000 UV/Vis and Spex Fluorolog 212 spectrometers were used for collecting the steady-state absorption and emission spectra in 1 cm quartz cuvettes. Time-resolved emission spectra were obtained by a combination of broadband fluorescence upconversion (FLUPS) and time-correlated single photon counting (TCSPC) techniques. FLUPS measurements used an amplified Ti:sapphire laser optical parametric amplifier which provided 400 nm excitation and 1340 nm gate pulses with 40 fs FWHM and 500 Hz repetition rate. Time-resolved spectra with 80 fs resolution and 1.8 ns time windows were collected at room

temperature, 20.5 ± 1 °C. The solutions, which had solute optical densities near 1 at 400 nm, were kept inside an argon-purged box and circulated through a 0.2 mm thickness optical cell. TCSPC data were excited by the doubled output of a Ti:sapphire laser also at 400 nm and recorded with a 25 ps (fwhm) instrument response function over a 20 ns window. Spectra were derived from the TCSPC data by spectral reconstruction using decays at 15-20 wavelengths referenced to the steady-state spectrum. The TCSPC samples were sealed in 1 cm quartz cuvettes and thermostated to 20.5 ± 0.1 °C. Both parallel and perpendicularly polarized emission decays were recorded with TCSPC in order to determine rotational correlation functions, as described in detail in Ref.[64].

Results and Discussion

A Solvation Response Functions

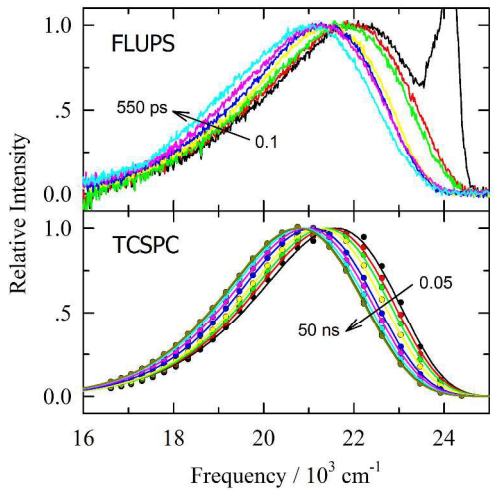

Fig.1 Representative time-resolved emission spectra of 4AP in $[Im_{41}][BF_4]$. The top panel shows FLUPS data and the lower panel lognormal fits (solid line) to reconstructed TCSPC spectra (points). The spike near 24,000 cm^{-1} in the earliest FLUPS spectrum is due to Raman scattering.

Representative time-resolved emission spectra of 4AP in $[Im_{41}][BF_4]$ are shown in Figure 1. By fitting spectra observed by both techniques to log-normal lineshape functions, the peak frequencies $\nu_{pk}(t)$ were determined and combined over the time range 100-600 ps.[35] The resulting $\nu_{pk}(t)$ of 4AP and corresponding C153 data in the four ILs surveyed are displayed in Figure 2. Both data sets show a clear biphasic solvation response, consisting of a fast component decaying within 1 ps, followed by a slow component extending up to a few nanoseconds. However there is much greater variation of ν_{pk} at long times in the case of 4AP and the Stokes shift involved in the fast response of 4AP is only half of that observed in C153.

From these peak frequency data, spectral response functions

$$S_\nu(t) = \frac{\nu_{pk}(t) - \nu_{pk}(\infty)}{\nu_{pk}(0) - \nu_{pk}(\infty)} \quad (1)$$

were constructed, where the values of $\nu_{pk}(0)$ were obtained from steady-state spectral estimates[65] and the $\nu_{pk}(\infty)$ from extrapolating TCSPC data to long times. Values of $\nu_{pk}(0)$ and $\nu_{pk}(\infty)$ are listed in Table 2 (C153 data are from Ref. 35). As discussed in our previous papers[35, 36], the fast component of $S_\nu(t)$ is associated with inertial motions whereas the slower component results from diffusive molecular dynamics. Although we expect solvent ion motions to primarily dictate the observed solvation response in these large solutes, solute dynamics are also mixed into both components[51, 57]. A Gaussian + stretched exponential function,

$$S_\nu(t) = f_G \exp\left\{-\frac{1}{2}\omega_G^2 t^2\right\} + (1-f_G)\exp\left\{-\left(\frac{t}{\tau}\right)^\beta\right\} \quad (2)$$

provides a good representation of these biphasic dynamics. Values of the fit parameters are compiled in Table 2. Also included in Table 2 are the integral times associated with the Gaussian and stretched components, calculated as $\langle\tau_G\rangle = (\pi/2)^{1/2}\omega_G^{-1}$ and $\langle\tau_{str}\rangle = \tau\Gamma(\beta^{-1})/\beta$, respectively. In contrast to C153, the less pronounced fast component (Fig. 2) leads to a smaller value of f_G and values of ω_G which are less well defined in the case of 4AP.

Of primary interest in the present work are the times associated with the slower solvation component $\langle\tau_{str}\rangle$, and the overall response times $\langle\tau_{solv}\rangle = f_G\langle\tau_G\rangle + (1-f_G)\langle\tau_{str}\rangle$. As seen from Table 2 these times are all larger for 4AP than for C153. To quantify the differences of integral solvation times $\langle\tau_{solv}\rangle$, between two probes "D1" and "D2" we use the fractional difference

$$\Delta\tau = \frac{2(\langle\tau_{solv}\rangle_{D2} - \langle\tau_{solv}\rangle_{D1})}{\langle\tau_{solv}\rangle_{D2} + \langle\tau_{solv}\rangle_{D1}} \quad (3)$$

Values of Δτ are collected in Table 2. They range from 19-59%.

Several groups have previously measured solvation response functions of C153 and 4AP with lower time resolution in some of the same solvents studied here.[45, 72-74] The present data are compared to these prior data in the Supporting Information.[47, 66-68]

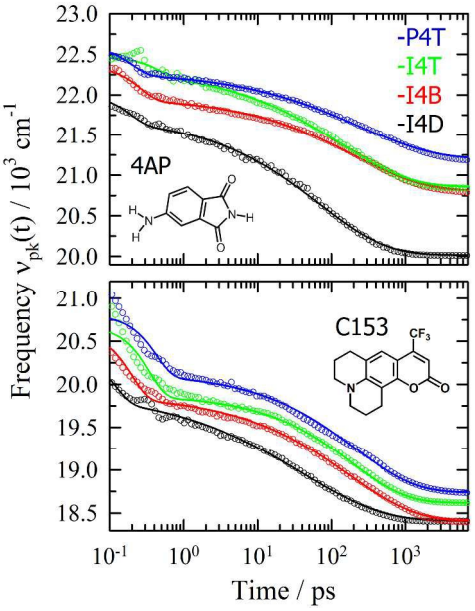

Fig.2 Peak frequency evolution $\upsilon_{pk}(t)$ (points) and of these data to eq.2 (curves) for C153 and 4AP in $[Pr_{41}][Tf_2N]$ (P4T), $[Im_{41}][Tf_2N]$ (I4T), $[Im_{41}][BF_4]$ (I4B) and $[Im_{41}][DCA]$ (I4T).

Table 1 Probes and Ionic Liquids Studied[α]

ID[(a)]	Dye / IL	CAS RN	chemical name	source	V_{vdW} / Å$^{3(b)}$
-	C153	53518-18-6	coumarin 153	Lambda Physik (>99%) / Exciton (laser grade)	243
-	4AP	3676-85-5	4-aminophthalimide	Acros (97%) / Aldrich (98%)	134
-	DCS	2844-17-9	trans-4-dimethylamino-4'-cyanostilbene	Klaas Zachariasse[69]	250
I4D	$[Im_{41}][DCA]$	448245-52-1	1-butyl-3-methylimidazolium dicyanamide	Iolitec (>98%)	104
I4B	$[Im_{41}][BF_4]$	174501-65-6	1-butyl-3-methylimidazolium tetrafluoroborate	Iolitec (99%)	97
I4T	$[Im_{41}][Tf_2N]$	174899-83-3	1-butyl-3-methylimidazolium bis(trifluoromethylsulfonyl)imide	Iolitec (99%)	155
I4P	$[Im_{41}][PF_6]$	174501-64-5	1-butyl-3-methylimidazoliumn hexafluorophosphate	Iolitec (99%)	112
P3T	$[Pr_{31}][Tf_2N]$	223437-05-6	1-propyl-1-methylpyrrolidinium bis(trifluoromethanesulfonyl)imide	Gary Baker[70]	155
P4T	$[Pr_{41}][Tf_2N]$	223437-11-4	1-butyl-1-methylpyrrolidinium bis(trifluoromethanesulfonyl)imide	Iolitec (99%)	164

(a) ID is the abbreviation used to designate dyes and ionic liquids throughout the paper. CAS RN is the Chemical Abstracts registry number. Probes from different sources were used in FLUPS and TCSPC measurements, respectively. (b) V_{vdW} are van der Waals volumes calculated using atomic increments from J. T. Edwards, *J. Chem. Ed.* (1970) **47**, 261-270. Values listed for the ionic liquids the averages of cation and anion values.

B Rotational Dynamics

4AP anisotropy data ($r(t)$) were recorded using both the FLUPS and TCSPC techniques. The FLUPS data did not show any components with time constants <10 ps, and in no cases was there more than a 10% decrease in $r(t)$ out to times of >100 ps. The FLUPS anisotropies were generally higher than those collected with TCSPC at times >200 ps, where we expect agreement between the two techniques (see Supporting Information). The early time amplitudes of the FLUPS data varied unsystematically (r_0 = 0.38±.05) among the different ionic liquids, presumably due to difficulties in accurately calibrating the polarization sensitivities of this experiment. For this reason we analyze only the TCSPC data here.

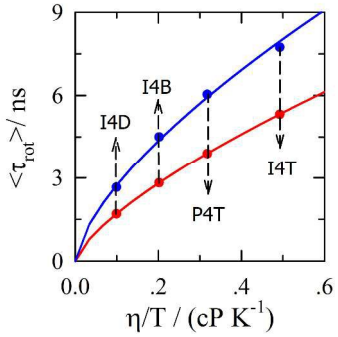

Fig. 3 Rotational correlation times of C153 (red dots) and 4AP (blue dots) as functions of solvent viscosity. "I4D", "I4B", "I4T" and "P4T" refer to ionic liquids $[Im_{41}][DCA]$, $[Im_{41}][BF_4]$, $[Im_{41}][Tf_2N]$ and $[Pr_{41}][Tf_2N]$, respectively. Smooth curves

are the power law fits $\langle\tau_{rot}\rangle/ns = 8.82(\eta/T)^{0.71}$ for C153 and $\langle\tau_{rot}\rangle/ns = 12.78(\eta/T)^{0.67}$ for 4AP.

Anisotropies measured at the peak of the steady-state spectrum and at the half-height points on its blue and red edges were the same to within anticipated uncertainties and we therefore report the average values. In general the anisotropy decays could be fit using a single stretched exponential function,

$$r(t) = r_0 \exp\left\{-(t/\tau_{rot})^{\beta_{rot}}\right\} \quad (4)$$

Fit parameters r_0, τ_{rot}, β_{rot} and the rotational correlation times $\langle\tau_{rot}\rangle$ are listed in Table 3. In the case of 4AP single exponential fits (β_{rot}=1) adequately represented $r(t)$ whereas for C153 significant non-exponentiality ($\beta_{rot}\leq$0.85) is observed. Note that the parameters of C153 reported here are from our previous study at 298 K[71] with a small temperature correction applied assuming that within a single solvent $\tau_{rot} \propto \eta/T$, where η is the solvent shear viscosity and T is the temperature in Kelvin.

As shown in Figure 3, rotational correlation times $\langle\tau_{rot}\rangle$ show a simple dependence on solvent viscosity, but contrary to hydrodynamic predictions, we find $\tau_{rot} \propto \eta^p$ with p significantly smaller than unity (p = 0.71 and 0.67 for C153 and 4AP, respectively) One way of describing such departures from the expected dependence $\tau_{rot} \propto \eta$ is to invoke solvent-dependent rotational coupling constants, $C_{rot} = \langle\tau_{rot}\rangle/\tau_{stk}$, where τ_{stk} is the hydrodynamic prediction using stick boundary conditions, $\tau_{stk} = V f_{stk}\eta/k_B T$, with V and f_{stk} the solute volume and shape factor. (Solute volumes are listed in Table 1 and values of f_{stk} based on ellipsoidal models are 1.6 for 4AP 1.5 for C153.[40]) In conventional solvents the coupling constants of 4AP have been previously reported to be C_{rot}~1 in aprotic solvents and C_{rot}~3 in alcohols,[40, 41] whereas for C153 values of C_{rot} <1 are observed with a systematic dependence of C_{rot} on the solvent molecule size.[72] C153 was also previously studied in a collection of 19 ionic liquids where C_{rot} was found to be 0.5±0.1.[73] For 4AP in the four ILs surveyed here, C_{rot} lies within the range measured in conventional solvents, closer to values reported in polar aprotic solvents. Considering the sizes of the ions in the ILs examine here, ($Im_{41}^+ \cong Pr_{41}^+$ and Tf_2N^- >>DCA^->BF4$^-$.[71]) no systematic dependence on ion size can be discerned.

Table 2 Summary of Peak Frequencies and Parameters Characterizing the Solvation Response[α]

4AP / IL	ν(0)/10^3 cm^{-1}	ν(∞)/10^3 cm^{-1}	f_G	ω_G/ps^{-1}	$\langle\tau\rangle_G$/ps	τ/ns	β	$\langle\tau\rangle_{str}$/ns	Δτ
I4D	22.38	20.81	0.33	15	0.08	0.06	0.45	0.15	19%
I4B	22.06	20.02	0.26	5.3	0.24	0.22	0.47	0.48	38%
I4T	22.52	20.86	0.12	2.8	0.45	0.13	0.46	0.32	45%
P4T	22.63	21.21	0.24	6.9	0.18	0.24	0.45	0.60	59%
C153 / IL	**ν(0)/10^3 cm^{-1}**	**ν(∞)/10^3 cm^{-1}**	f_G	ω_G/ps^{-1}	$\langle\tau\rangle_G$/ps	τ/ns	β	$\langle\tau\rangle_{str}$/ns	Δτ
I4D	20.48	18.41	0.32	6.9	0.18	0.05	0.44	0.12	-
I4B	20.63	18.41	0.34	7	0.18	0.17	0.48	0.37	-
I4T	20.68	18.62	0.39	4.1	0.31	0.19	0.6	0.29	-
P4T	20.82	18.74	0.33	3.3	0.38	0.21	0.54	0.37	-

[α]ν(0) and ν(∞) denote the peak frequencies of the "time-zero" emission and the extrapolated value of the time-dependent emission spectrum, respectively. f_G, ω_G, β and τ are the fit parameters of eq. 2 used to describe $S_\nu(t)$. $\langle\tau\rangle_G$ and $\langle\tau\rangle_{str}$ are the integral times of Gaussian and stretched exponential components of $S_\nu(t)$, respectively. Δ, quantifies the difference between integral solvation times reported by the two probes according to eq. 3.

C The Rotationally Corrected Solvation Response

In prior experimental studies of solvation dynamics, solute motion has usually been assumed to be of minor importance and therefore ignored, especially in conventional dipolar solvents.[74] Early simulations in conventional solvents showed that rotation of a small solute such as benzene does influence solvation dynamics, and it was thought that this effect should be minimal for a large solute like C153 in small-molecule solvents such as methanol and acetonitrile.[75] In contrast, simulations in ILs point out that solute motion can significantly accelerate solvation dynamics. Early simulations showed that pronounced effects of solute motion can occur with small solutes, due to the possibility of rapid large-angle

Table 3 Parameters Characterizing the Anisotropy Response[α]

4AP / IL	r_0	β_r	τ_r/ ns	$\langle\tau_{rot}\rangle$/ ns	C_{rot}
I4D	0.29	1	2.66	2.66	1.69
I4B	0.30	1	7.74	7.74	1.10
I4T	0.30	1	4.50	4.50	1.38
P4T	0.28	1	6.04	6.04	1.20
C153 / IL	r_0	β_r	τ_r/ ns	$\langle\tau_{rot}\rangle$/ ns	C_{rot}
I4D	0.38	0.85	1.70	1.85	0.58
I4B	0.38	0.76	5.32	6.27	0.46
I4T	0.38	0.77	2.82	3.29	0.49
P4T	0.38	0.71	3.89	4.86	0.50

[α]Rotational correlation function r(t) is characterized with fit parameters r_0, β_r and τ_r using eq. 4. C_{rot} is the rotational coupling factor defined by $C_{rot} = \langle\tau_{rot}\rangle / \tau_{stk}$

rotational jumps.[49, 76] More recent simulations have shown that solute motion can be quite significant even in the case of large solutes like C153.[77] Whereas in dipolar solvents, rotational solute motion should account for most of the effect, in ILs both rotational and translational solute motions can participate in solvation. The results of a semi-molecular theory of solvation also predicts significant effects of solute motion on the long but not the short components of solvation in ionic liquids.[78] The relative importance of rotational versus translational solute motions remains unclear at this point.

Sajadi et al.[79] recently used FLUPS to measure solvation and rotational dynamics of four chromophores, including C153 and 4AP, in methanol. They observed significant variations of solvation time with solute, variations which were roughly correlated to the solute rotation times. Using the idea that the observed solvation response $S_v(t)$ can be approximated by a product of the response of the solvent alone times a function describing the influence of solute motion,[75] they found that consistent times among the collection of solutes could be obtained by "correcting" $S_v(t)$ by the rotational correlation function

$$C_r^{(2)}(t) = r(t)/r_0 \qquad (5)$$

using

$$S_{RC}(t) = S_v(t)/\{C_r^{(2)}(t)\}^p \qquad (6)$$

"RC" here stands for "rotationally corrected" with the implication that this response function is now due to solvent motion alone. Sajadi et al. found that allowing p to vary between 0-1.4 provided a universal $S_{RC}(t)$ curve for four assorted solutes.

In the present work, we use this same approach to examine whether the systematic difference in solvation times between 4AP and C153 may be attributed to differences in solute motion. For this purpose we use eq. 6 with p=1 to calculate rotationally corrected solvation response functions. Parameters of $S_{RC}(t)$ fitted to eq.2 are collected in Table S1 (Supporting Information). ΔRC is used to quantify the change of solvation time caused by the rotational correction,

$$\Delta RC = \frac{\langle\tau_{solv}\rangle_{RC} - \langle\tau_{solv}\rangle}{\langle\tau_{solv}\rangle} \qquad (7)$$

As indicated in Table S1, the effect of the rotational correction is almost negligible in the case of 4AP (an average of 3%) whereas the faster rotation of C153 leads to the correction having a much more significant effect, which averages 31%.

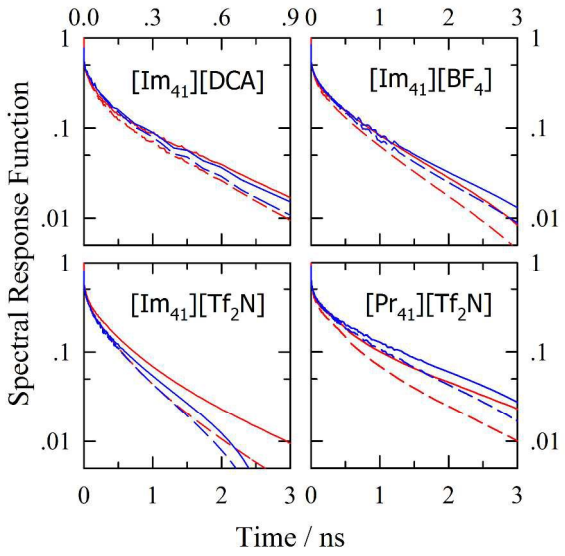

Fig. 4 Representative spectral response functions $S_v(t)$ (dashed lines) and their rotationally corrected versions, $S_{RC}(t)$ (solid lines) of C153 (red) and 4AP (blue). Both $S_v(t)$ and $S_{RC}(t)$ of 4AP are normalized to those of C153 at 2 ps.

In Figures 4 and 5 we compare the measured solvation response functions and their rotationally corrected versions, after a rescaling of the 4AP data. Due to ambiguities in the $\nu_{pk}(0)$ estimates, the early-time dynamics of solvation measured for 4AP are not determined as well as those of C153. In addition, we anticipate the inertial dynamics may be more

solute and perhaps solvent specific. Therefore, in order to focus more on the slower portions of the dynamics, the response functions of 4AP are normalized to those of C153 at 2 ps in Figures 4 and 5. These two figures contain the same data in two different semi-logarithmic formats which emphasize different aspects of the data. Figure 4 indicates that the rotational correction substantially reduces the differences between the solvation response functions obtained with C153 and 4AP. The good overall agreement between the rotationally corrected response functions in both figures validates this treatment.

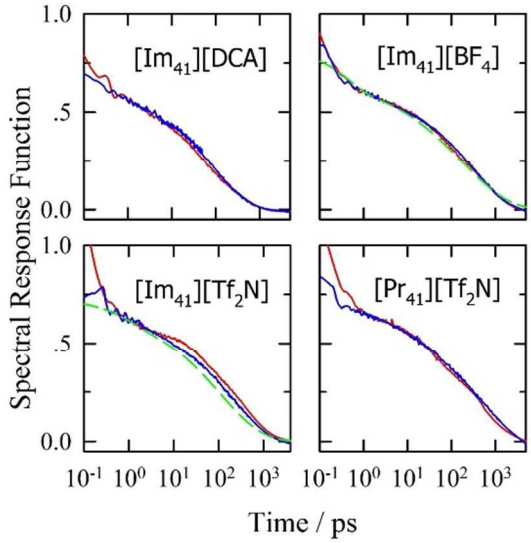

Fig. 5 RC corrected spectral response function $S_{RC}(t)$ of C153 (red) and 4AP (blue). Uncorrected response functions ($S_v(t)$) of DCS (green dashed curves) measured at 298 K from Ref.[38] are also shown. The 4AP and DCS data are is normalized to C153 at t=2ps and used for reference as an 'immobile' solute.

Ultrafast data on a third solvatochromic probe, trans-4-dimethylamino-4'-cyanostilbene (DCS), [38, 40 80-82] is included in Figure 5 to further support the idea that solute motions are responsible for the differences in observed $S_v(t)$ functions. Prior work[38] has shown that the elongated shape of DCS (f_{stk}=2.8) makes its rotation times much slower than those of either C153 or 4AP. Thus, DCS might be expected to represent a case wherein rotational motion is unimportant, even in ionic liquids. Indeed, we find that rotation times are so slow as to have a negligible effect when applied in the manner done for 4AP and C153. Data from prior Kerr-gated emission measurements of DCS[36] are therefore shown without rotational correction in Figure 5 (green dashed curves). Details of these comparisons are provided in the Supporting Information. Here we simply comment that for the two direct comparisons we can make, Figure 5 shows there is excellent agreement between the rotationally corrected 4AP and C153 data and the uncorrected DCS data in the case of $[Im_{41}][BF_4]$ and much less impressive agreement in $[Im_{41}][Tf_2N]$.

Finally it should be noted that this rotational correction ignores the influence of solute translation. Simulations suggest that contributions from rotational and translational motions of C153 play nearly equal roles in its solvation.[77] The fact that we consider only rotation here may mean that we overemphasize the rotational aspect of the problem.

D Dielectric Continuum Models of Solvation

We now consider the relevance of the above results to testing the validity of continuum models of solvation. In our recent work we have made extensive comparisons between solvation response functions measured with C153 to predictions made using dielectric dispersion data $\hat{\varepsilon}(\nu)$ on the neat solvent and a simple dielectric continuum model of solvation.[35, 36, 83, 84] In making these comparisons no account was made for the possible effects of solute motion on the observed dynamics. A simple place to examine the effect of solute motion is in the predicted relationship between integral solvation times $\langle\tau_{solv}\rangle$ and the DC conductivity σ_0 [83, 84]

$$\langle\tau_{solv}\rangle = (n_D^2 + \tfrac{1}{2}\varepsilon_c)/4\pi\sigma_0 \cong const/\sigma_0 \qquad (8)$$

In this expression n_D is the solvent refractive index and ε_C (= 2 here) is a cavity dielectric constant used to account for solute polarizability. Because the refractive indices of ionic liquids vary negligibly compared to their conductivities, the integral solvation time predicted by eq. 8 is essentially proportional to solution resistivity σ_0^{-1}. We previously examined the accuracy of eq.8 using data from 38 measurements on C153 in 34 different ILs[84], and found that these data can be approximately represented by the power law

$$\ln\left(\langle\tau_{solv}\rangle/\text{ps}\right) = 4.37 - 0.92\ln\left(\sigma_0/\text{S m}^{-1}\right) \qquad (9)$$

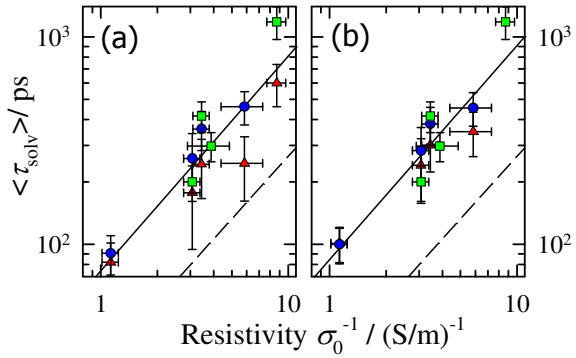

Fig. 6 Integral solvation times of 4AP (blue circle), C153 (red triangle) and DCS (green square) versus solvent resistivity. The surveyed ionic liquids include $[Im_{41}][DCA]$, $[Im_{41}][BF4]$, $[Im_{41}][Tf_2N]$, $[Im_{41}][PF_6]$, $[Pr_{31}][Tf_2N]$ and $[Pr_{41}][Tf_2N]$. (a) original experimental data (b) rotationally corrected data. The dashed lines in both panels are the dielectric continuum prediction (eq.8) and the solid lines the fits of the data to the functional form of eq.9.

Figure 6 compares $\langle\tau_{solv}\rangle$ to solvent resistivity σ_0^{-1} for the four ILs examined in this work and two additional ILs ($[Im_{41}][PF_6]$ and $[Pr_{31}][Tf_2N]$) surveyed in the previous DCS work.[38] The dashed and solid lines in these plots are respectively the dielectric continuum predictions (eq.8) and fits

to the form of eq. 9 using these more limited sets of data. Figure 6 shows that application of the rotational correction changes the observed correlation and its relationship to the dielectric continuum prediction by only a modest amount. The main effect of rotational correction is to reduce scatter of the data (R^2 = 0.82 and 38% error versus 0.87 and 28% error after correction) and to worsen the disagreement with continuum predictions by a modest amount (~13% out of an error of a factor of ~3).

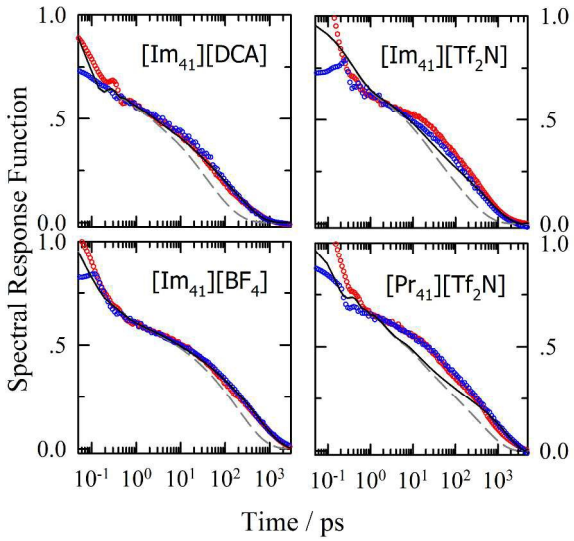

Fig. 7 Continuum model prediction with experimental and fitted conductivity are showed in gray dashed and black solid line. The red and blue dots are $S_{RC}(t)$ of C153 and 4AP (with normalization to C153 at 2 ps).

Although the overall solvation times are not predicted by the dielectric continuum model, we showed previously that the shapes of the predicted $S_v(t)$ response functions compare well with those observed with C153.[35] We also showed that using the dielectric response measured in experiment and allowing the static conductivity to serve as an adjustable parameter which serves to scale the overall solvation time, the observed and predicted $S_v(t)$ can typically be brought into good agreement.[83] Figure 7 shows that the same is true when rotationally corrected data are used for such comparisons. Here the rotationally corrected data for both C153 and (scaled data) for 4AP are compared to dielectric continuum predictions using both measured conductivities (dashed black curves) and conductivities fit to match $\langle\tau_{solv}\rangle$ of C153. As indicated by Fig. 6, the conductivities needed to accomplish this fitting are a factor of ~0.63 smaller than experimental values. The agreement achieved is better in the case of [Im_{41}][DCA] and [Im_{41}][BF_4], the liquids with the smaller anions.

Conclusions

We have studied the solvation and rotational dynamics of 4AP in four ionic liquids using a combination of FLUPS + TCSPC. Comparing the observed solvation response functions with prior results obtained with the probe C153 enables us to investigate the effect of solute motion on solvation dynamics. The main conclusions of this work may be summarized as follows:

1 Solvation dynamics of 4AP in ILs is biphasic and similar to what was reported previously with C153. The integral solvation times $\langle\tau_{solv}\rangle$ reported by 4AP are systematically larger than those of C153, by an average of 33%.

2 No fast anisotropy components of 4AP are observed in FLUPS experiments, enabling the use of TCSPC anisotropies for measuring the rotational correlation functions of these probes in ILs. The rotation of 4AP is significantly slower than that C153, by an average factor of 1.32. The opposite is predicted by hydrodynamic calculations, which predict substantially faster rotation of the smaller 4AP. The rotational coupling constants C_{rot} of 4AP in the four ILs studied here lie between the values previously measured in aprotic (~1) and alcohol (~2.7) solvents[40] and do not show a systematic dependence on ion size in ILs.

3 We have tested the idea that solute motion may speed the solvation response in ionic liquids by applying the rotational correction (RC) proposed by Sajadi et al.[79] This correction consists of dividing the observed solvation response function by the rotational correlation function determined from anisotropy data. Results show that application of such a correction reduces the average difference in solvation times of 4AP and C153 by ~23%. Literature data on the chromophore DCS,[38] which has much longer rotation times than either C153 or 4AP, support the idea that consistency among probes may be improved using this approach. It should be noted, however, that both rotational and translational motions of the solute play a role in ionic liquid solvation. The rotational correction only addresses the first of these effects.

4 Prior comparisons of the solvation response to dielectric continuum predictions assumed no contribution from solute motion.[83, 84] The more proper comparisons made using rotationally corrected data worsens the agreement with continuum predictions, which were already too fast compared to experiment. This discrepancy and the effect of solute motion parallel the behavior reported earlier using computer simulations.[36]

Acknowledgement

J.B. and M.M. acknowledge financial support of this work from Division of Chemical Sciences, Geosciences, and Biosciences, Office of Basic Energy Sciences of the U.S. Department of Energy through grant DE-FG02-12ER16363. X.-X.Z. and N.P.E. were supported by the Deutsche Forschungsgemeinschaft (priority program "Ionic Liquids") X.-X.Z. is also grateful for financial support by the NSFC (21373232) during the later stage of her work.

Notes

a Beijing National Laboratory for Molecular Sciences, Institute of Chemistry, Chinese Academy of Sciences, Beijing 100190, P. R. China.
b Department of Chemistry, Humboldt Universität zu Berlin, Berlin 12489, Germany.
c Department of Chemistry, The Pennsylvania State University, University Park, PA, USA.
*Corresponding authors: xinxingzhang@iccas.ac.cn. and maroncelli@psu.edu

Notes and References

1. M. J. Earle and K. R. Seddon, *Pure Appl. Chem.*, 2000, **72**, 1391-1398.
2. J. H. Davis, *Chem. Lett.*, 2004, **33**, 1072-1077.
3. R. Kawano, T. Katakabe, H. Shimosawa, M. K. Nazeeruddin, M. Graetzel, H. Matsui, T. Kitamura, N. Tanabe and M. Watanabe, *Phys. Chem. Chem. Phys.*, 2010, **12**, 1916-1921.
4. S. M. Zakeeruddin and M. Gratzel, *Adv. Funct. Mater.*, 2009, **19**, 2187-2202.
5. A. Lewandowski and A. Swiderska, *Applied Physics A: Materials Science & Processing*, 2006, **82**, 579-584.
6. P. Wasserscheid and T. Welton, eds., *Ionic Liquids in Synthesis*, Wiley-VCH, Weinheim, 2003.
7. J. Wishart, *J. Phys. Chem. Lett.*, 2010, **1**, 1629-1630.
8. A. Stark, *Top. Curr. Chem.*, 2009, **290**, 41-81.
9. J. P. Hallett and T. Welton, *Chem. Rev.*, 2011, **111**, 3508-3576.
10. P. Sun and D. W. Armstrong, *Anal. Chim. Acta*, 2010, **661**, 1-16.
11. H. Tadesse and R. Luque, *Energy & Environmental Science*, 2011, **4**, 3913-3929.
12. M. Armand, F. Endres, D. R. MacFarlane, H. Ohno and B. Scrosati, *Nat. Mater.*, 2009, **8**, 621-629.
13. R. Y. Lin, P. L. Taberna, S. Fantini, V. Presser, C. R. Perez, F. Malbosc, N. L. Rupesinghe, K. B. K. Teo, Y. Gogotsi and P. Simon, *J. Phys. Chem. Lett.*, 2011, **2**, 2396-2401.
14. J. Dupont, R. F. de Souza and P. A. Z. Suarez, *Chem. Rev.*, 2002, **102**, 3667-3691.
15. R. D. Rogers and K. R. Seddon, *Science*, 2003, **302**, 792-793.
16. T. Torimoto, T. Tsuda, K. Okazaki and S. Kuwabata, *Adv. Mater.*, 2010, **22**, 1196-1221.
17. S. Schröedle, G. Annat, D. R. MacFarlane, M. Forsyth, R. Buchner and G. Hefter, *Chem. Commun.*, 2006, 1748-1750.
18. A. Stoppa, J. Hunger, R. Buchner, G. Hefter, A. Thoman and H. Helm, *J. Phys. Chem. B*, 2008, **112**, 4854-4858.
19. O. Zech, A. Stoppa, R. Buchner and W. Kunz, *J. Chem. Eng. Data*, 2010, **55**, 1774-1778.
20. H. Weingaertner, *Angew. Chem. Int. Ed.*, 2007, **46**, 2-19.
21. M. Krueger, E. Bruendermann, S. Funkner, H. Weingaertner and M. Havenith, *J. Chem. Phys.*, 2010, **132**, 101101/101101-101101/101104.
22. M. Mizoshiri, T. Nagao, Y. Mizoguchi and M. Yao, *J. Chem. Phys.*, 2010, **132**, 164510/164511-164510/164517.
23. K. Nakamura and T. Shikata, *ChemPhysChem*, 2010, **11**, 285-294.
24. D. A. Turton, T. Sonnleitner, A. Ortner, M. Walther, G. Hefter, K. R. Seddon, S. Stana, N. V. Plechkova, R. Buchner and K. Wynne, *Faraday Discuss.*, 2012, **154**, 145-153.
25. Z. Ren, A. S. Ivanova, D. Couchot-Vore and S. Garrett-Roe, *J. Phys. Chem. Lett.*, 2014, **5**, 1541-1546.
26. A. Samanta, *J. Phys. Chem. Lett.*, 2010, **1**, 1557-1562.
27. N. Ito and R. Richert, *J. Phys. Chem. B*, 2007, **111**, 5016-5022.
28. H. Jin, G. A. Baker, S. Arzhantsev, J. Dong and M. Maroncelli, *J. Phys. Chem. B*, 2007, **117**, 7291-7302.
29. A. M. Funston, T. A. Fadeeva, J. F. Wishart and E. W. Castner, *J. Phys. Chem. B*, 2007, **111**, 4963-4977.
30. S. K. Das and M. Sarkar, *J. Lumin.*, 2012, **132**, 368-374.
31. P. J. Carlson, S. Bose, D. W. Armstrong, T. Hawkins, M. S. Gordon and J. W. Petrich, *J. Phys. Chem. B*, 2012, **116**, 503-512.
32. Y. Nagasawa, A. Oishi, T. Itoh, M. Yasuda, M. Muramatsu, Y. Ishibashi, S. Ito and H. Miyasaka, *Journal of Physical Chemistry C*, 2009, **113**, 11868-11876.
33. E. W. Castner, J. F. Wishart and H. Shirota, *Acc. Chem. Res.*, 2007, **40**, 1217-1227.
34. H. Fukazawa, T. Ishida and H. Shirota, *J. Phys. Chem. B*, 2011, **115**, 4621-4631.
35. X.-X. Zhang, M. Liang, N. P. Ernsting and M. Maroncelli, *J. Phys. Chem. B*, 2013, **117**, 4291-4304.
36. M. Maroncelli, X. X. Zhang, M. Liang, D. Roy and N. P. Ernsting, *Faraday Discuss.*, 2012, **154**, 409-424.
37. B. Lang, G. Angulo and E. Vauthey, *J. Phys. Chem. A*, 2006, **110**, 7028-7034.
38. S. Arzhantsev, H. Jin, G. A. Baker and M. Maroncelli, *J. Phys. Chem. B*, 2007, **111**, 4978-4989.
39. M. Muramatsu, Y. Nagasawa and H. Miyasaka, *J. Phys. Chem. A*, 2011, **115**, 3886-3894.
40. N. Ito, S. Arzhantsev and M. Maroncelli, *Chem. Phys. Lett.*, 2004, **396**, 83-91.
41. J. A. Ingram, R. S. Moog, N. Ito, R. Biswas and M. Maroncelli, *J. Phys. Chem. B*, 2003, **107**, 5926-5932.
42. D. C. Khara and A. Samanta, *Phys. Chem. Chem. Phys.*, 2010, **12**, 7671-7677.
43. A. Paul and A. Samanta, *J. Phys. Chem. B*, 2008, **112**, 947-953.
44. K. Fruchey and M. D. Fayer, *J. Phys. Chem. B*, 2010, **114**, 2840-2845.
45. R. Karmakar and A. Samanta, *J. Phys. Chem. A*, 2002, **106**, 6670-6675.
46. G. B. Dutt, *J. Phys. Chem. B*, 2010, **114**, 8971-8977.
47. R. Karmakar and A. Samanta, *J. Phys. Chem. A*, 2003, **107**, 7340-7346.
48. Y. Nagasawa and H. Miyasaka, *Phys. Chem. Chem. Phys.*, 2014, **16**, 13008-13026.
49. Y. Shim, J. Duan, M. Y. Choi and H. J. Kim, *J. Chem. Phys.*, 2003, **119**, 6411-6414.
50. Y. Shim, M. Y. Choi and H. J. Kim, *J. Chem. Phys.*, 2005, **122**, 044511.
51. Y. Shim and H. J. Kim, *J. Phys. Chem. B*, 2008, **112**, 11028-11038.
52. Y. Shim and H. J. Kim, *J. Phys. Chem. B*, 2013, **117**, 11743-11752.
53. R. M. Lynden-Bell, *J. Phys. Chem. B*, 2007, **111**, 10800-10806.
54. M. N. Kobrak and V. Znamenskiy, *Chem. Phys. Lett.*, 2004, **395**, 127-132.
55. M. N. Kobrak, *J. Chem. Phys.*, 2006, **125**, 64502.
56. M. N. Kobrak, *J. Chem. Phys.*, 2007, **127**, 099903/099901.
57. D. Roy and M. Maroncelli, *J. Phys. Chem. B*, 2012, **116**, 5951-5970.
58. Z. L. Terranova and S. A. Corcelli, *J. Phys. Chem. B*, 2013, **117**, 15659-15666.
59. M. Schmollngruber, C. Schroeder and O. Steinhauser, *J. Chem. Phys.*, 2013, **138**, 204504.
60. M. Schmollngruber, C. Schroeder and O. Steinhauser, *Phys. Chem. Chem. Phys.*, 2014, **16**, 10999-11009.
61. D. Jeong, M. Y. Choi, Y. Jung and H. J. Kim, *J. Chem. Phys.*, 2008, **128**, 174504/174501-174504/174507.
62. S. Daschakraborty, T. Pal and R. Biswas, *J Chem Phys*, 2013, **139**, 164503.
63. M. Sajadi, M. Weinberger, H.-A. Wagenknecht and N. P. Ernsting, *Phys Chem Chem Phys*, 2011, **13**, 17768-17774.
64. N. Ito, S. Arzhantsev, M. Heitz and M. Maroncelli, *J. Phys. Chem. B*, 2004, **108**, 5771-5777.
65. R. S. Fee and M. Maroncelli, *Chem. Phys.*, 1994, **183**, 235-247.
66. R. Karmakar and A. Samanta, *J. Phys. Chem. A*, 2002, **106**, 4447-4452.
67. A. Samanta, *J. Phys. Chem. B*, 2006, **110**, 13704-13716.
68. P. K. Chowdhury, M. Halder, L. Sanders, T. Calhoun, J. L. Anderson, D. W. Armstrong, X. Song and J. W. Petrich, *J. Phys. Chem. B*, 2004, **108**, 10245-10255.
69. Y. V. Ilichev and K. A. Zachariasse, *Ber Bunsen Phys Chem*, 1997, **101**, 625-635.
70. S. N. Baker, T. M. McCleskey, S. Pandey and G. A. Baker, *Chem. Commun.*, 2004, 940-941.
71. H. Jin, G. A. Baker, S. Arzhantsev, J. Dong and M. Maroncelli, *J. Phys. Chem. B*, 2007, **111**, 7291-7302.

72. M. L. Horng, J. A. Gardecki and M. Maroncelli, *J. Phys. Chem. A*, 1997, **101**, 1030-1047.
73. H. Jin, X. Li and M. Maroncelli, *J. Phys. Chem. B*, 2007, **111**, 13473-13478
74. B. Bagchi, D. W. Oxtoby and G. R. Fleming, *Chem. Phys.*, 1984, **86**, 257-267.
75. P. V. Kumar and M. Maroncelli, *J. Chem. Phys.*, 1995, **103**, 3038-3060.
76. Y. Shim, D. Jeong, S. Manjari, M. Y. Choi and H. J. Kim, *Acc. Chem. Res.*, 2007, **40**, 1130-1137.
77. D. Roy and M. Maroncelli, *J. Phys. Chem. B*, 2012, **116**, 5951-5970.
78. S. Daschakraborty, T. Pal and R. Biswas, *J. Chem. Phys.*, 2013, **139**, 164503.
79. M. Sajadi, M. Weinberger, H. A. Wagenknecht and N. P. Ernsting, *Phys. Chem. Chem. Phys.*, 2011, **13**, 17768-17774.
80. Y. V. IIlchev, W. Kuhnle and K. A. Zachariasse, *Chem. Phys.*, 1996, **211**, 441-453.
81. S. Arzhantsev, H. Jin, G. A. Baker, N. Ito and M. Maroncelli, in *Femtochemistry VII, Ultrafast Processes in Chemistry, Physics, and Biology*, eds. A. W. Castleman and M. L. Kimble, Elsevier B.V., 2006, pp. 225-234.
82. H. El-Gezawy and W. Rettig, *Chem. Phys.*, 2006, **327**, 385-394.
83. X.-X. Zhang, C. Schroeder and N. P. Ernsting, *J. Chem. Phys.*, 2013, **138**, 111102.
84. X.-X. Zhang, M. Liang, N. P. Ernsting and M. Maroncelli, *J. Phys. Chem. Lett.*, 2013, **4**, 1205-1210.

